Received: 6 March 2020 | Revised: 18 June 2020 | Accepted: 22 June 2020

DOI: 10.1002/ardp.202000069

FULL PAPER

DPhG ARCH PHARM Archiv der Pharmazie

Novel 2-cyanoacrylamido-4,5,6,7-tetrahydrobenzo[*b*]thiophene derivatives as potent anticancer agents

Farid M. Sroor[1] | Mohamad M. Aboelenin[2] | Karima F. Mahrous[2] | Khaled Mahmoud[3] | Ahmed H. M. Elwahy[4] | Ismail A. Abdelhamid[4]

[1]Organometallic and Organometalloid Chemistry Department, National Research Centre, Cairo, Egypt

[2]Cell Biology Department, National Research Centre, Dokki, Giza, Egypt

[3]Pharmacognosy Department, National Research Centre, Dokki, Egypt

[4]Chemistry Department, Faculty of Science, Cairo University, Giza, Egypt

Correspondence
Farid M. Sroor, Organometallic and Organometalloid Chemistry Department, National Research Centre, Cairo 12622, Egypt.
Email: faridsroor@gmx.de and fm.sroor@nrc.sci.eg (F. M. S.)

Ahmed H. M. Elwahy and Ismail A. Abdelhamid, Department of Chemistry, Faculty of Science, Cairo University, Giza 12613, Egypt.
Email: aelwahy@yahoo.com (A. H. M. E.) and ismail_shafy@yahoo.com (I. A. A.)

Abstract

Ethyl 2-acrylamido-4,5,6,7-tetrahydrobenzo[*b*]thiophene-3-carboxylate as well as its corresponding *bis*-derivatives, **5**–**10**, with aliphatic linkers were synthesized, fully characterized, and tested as novel anticancer agents. The targeted compounds, **5**–**10**, were obtained by the Knoevenagel condensation reactions of *bis*-*o*- or -*p*-aldehyde with a molar ratio of ethyl 2-(2-cyanoacetamido)-4,5,6,7-tetrahydrobenzo[*b*]thiophene-3-carboxylate of **2** in the presence of piperidine in excellent yields (93–98%). The in vitro anticancer activities of the prepared compounds were evaluated against HepG2, MCF-7, HCT-116, and BJ1 cells. Compounds **7** and **9** emerged as the most promising compounds, with IC_{50} values of 13.5 and 32.2 μg/ml, respectively, against HepG2 cells, compared with the reference drug doxorubicin (IC_{50}: 21.6 μg/ml). Real-time reverse-transcription polymerase chain reaction was used to measure the changes in expression levels of the COL10A1 and COL11A1, ESR1, and ERBB2, or AXIN1 and CDKN2A genes within the treated cells, as genetic markers for colon, breast, or liver cancers, respectively. Treatment of the colon cancer cells with compounds **5**, **9**, and **10**, or breast and liver cancers cells with compounds **7**, **8**, **9**, and **10** downregulated the expression of the investigated tumor markers. The DNA damage values (depending on comet and DNA fragmentation assays) increased significantly upon treatment of colon cancer cells with compounds **5**, **9**, and **10**, and breast and liver cells with compounds **8**, **9**, and **10**. The structure–activity relationship suggested that the increase of the chain of the alkyl linker increases the anticancer activity and the compounds with *bis*-cyanoacrylamide moieties are more active than those with one cyanoacrylamide moiety.

KEYWORDS

2-cyanoacrylamide linked to 4,5,6,7-tetrahydrobenzo[*b*]thiophene, alkyl linkers, anticancer, bis(aromatic aldehydes), DNA damage, DNA fragmentation, gene expression

1 | INTRODUCTION

Cancer is one of the main causes of major morbidity and mortality worldwide, leading to a high percentage of deaths annually, as reported by the World Health Organization (WHO).[1] Therefore, it is of prime importance to develop novel and potent anticancer agents to fight against cancer, which is the hot topic in the research area nowadays. Thiophene and their fused derivatives are substantial building blocks and synthons in synthetic chemistry (Figure 1). The chemistry of these molecules is of increasing interest, as they seem to be promising pharmacological compounds with anticancer,[2-4] anti-inflammatory,[5,6] antibacterial (**I**),[7-9] antiproliferative,[10] antitubercular,[11] and antiviral

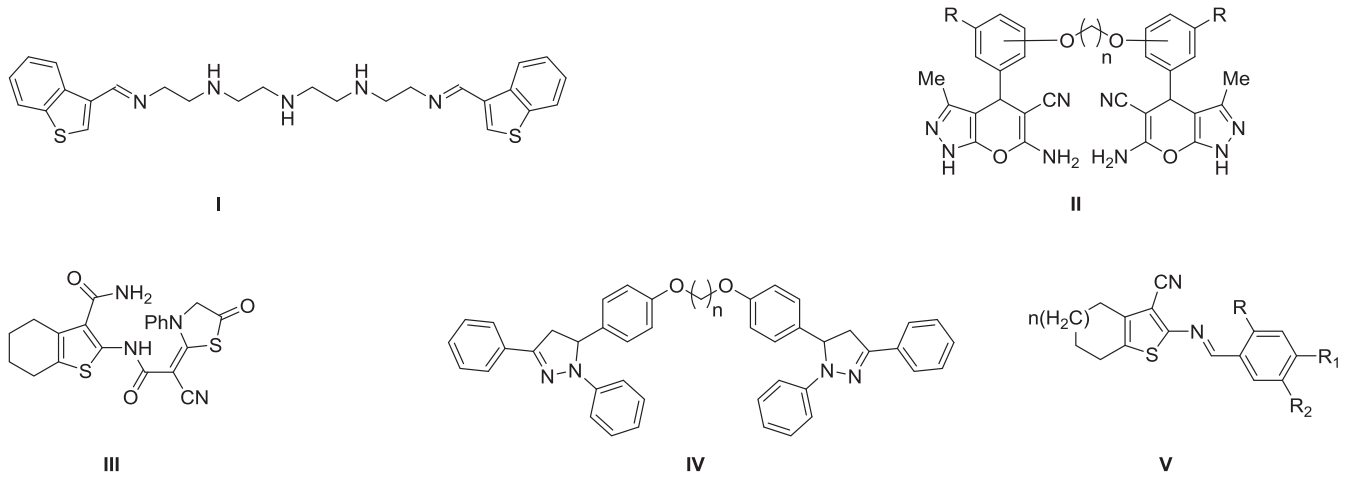

FIGURE 1 Examples of bioactive compounds containing the thiophene moiety and bioactive *bis*-heterocycles with ether linkers

properties.[12,13] Moreover, the acrylamide derivatives have attracted special attention due to their diverse biological and pharmacological applications such as anticancer (**II**),[14-16] anti-inflammatory (**III**),[17,18] antidiabetic,[19] antifungal,[20,21] and antimicrobial (**IV**) applications.[9,22,23]

In 2016, Aguiar et al.[24] reported a series of 2-aminothiophene derivatives, **V**, revealing their antiproliferative activity (Figure 1). The activity of these compounds has been evaluated against HeLa, PANC-1, and 3T3 cells, which were exposed to the compounds at concentrations of 5, 10, 25, or 50 μM for 24 or 48 hr. It was noted that nontumor fibroblast cells (3T3) were protected by treatment with the synthesized 2-aminothiophene derivatives and a pronounced proliferative effect was observed, particularly after 48 hr, suggesting greater neoplastic antiproliferative selectivity. Likewise, in the same period, the reference drug doxorubicin was more toxic than the selected 2-aminothiophene derivatives, which displayed a cell proliferation effect of <50%.[24]

However, a few studies have been performed on the use of *bis*-benzaldehydes as a starting material for the preparation of novel compounds with different applications such as redox flow battery,[25] biofunctional dynamic covalent polymer,[26] allosteric effectors of hemoglobin,[27] fluorescence-based assay,[28] in Groebke–Blackburn–Bienayme/Ugi reactions,[29] electrical conductivity,[30] macrocyclization,[31] breaking and mending of the porphyrin,[32] and a broad spectrum of biological activities.[16,23]

It is expected that the combination of tetrahydrobenzo[*b*]thiophene, acrylamide, and the alkyl linkers will increase the biological profile of the targeted compounds. It is worth to mention that the hydrophilic region in the targeted structures is homogeneously inside the cell and represents a suitable probe for viscosity measurements in the cytoplasm, whereas the hydrophobic region behaves as a membrane layer to some extent. However, the hydrophobic region also crosses the cell membrane and likely binds to intracellular proteins,[33] as explained in Figure 2.

In our endeavor toward the development and discovery of novel potent anticancer agents and in continuation of our previous work to

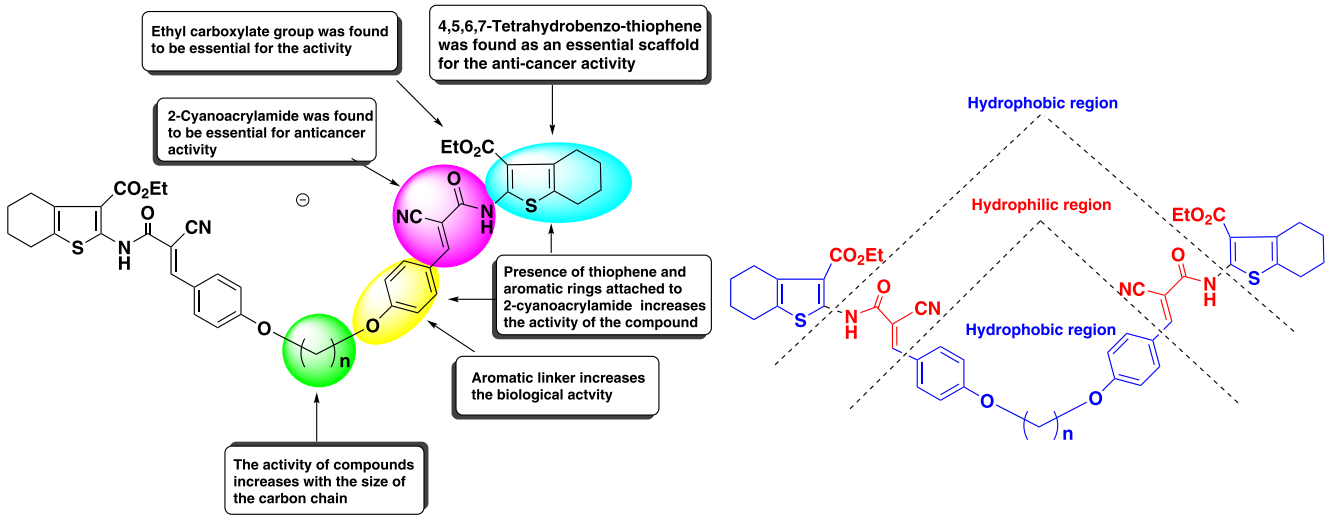

FIGURE 2 The design concept used for the synthesis of the title compounds

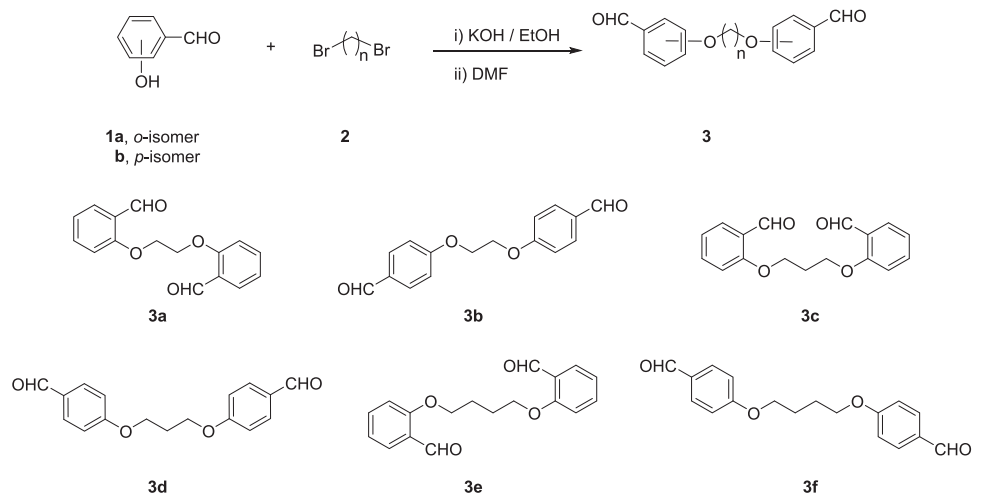

SCHEME 1 The synthesis of the bis(benzaldehydes) **3a–f**

prepare biologically active organic and organometallic compounds,[34-43] we decided to design and prepare a novel series of *bis*-(ethyl-2-(2-cyanoacrylamido)-4,5,6,7-tetrahydrobenzo[*b*]thiophene-3-carboxylates) utilizing the appropriate *bis*-aldehydes bearing aliphatic chain linkers as precursors (Figure 2).

2 | RESULTS AND DISCUSSION

2.1 | Chemistry

The key starting materials, bis(benzaldehydes) **3a–f**, were prepared, as reported by our group, through the reaction of the potassium salt of the appropriate hydroxybenzaldehydes **1a**,**b** with the corresponding dibromo compound **2** in dimethylformamide at reflux, as described in Scheme 1.[44-47] When the bis(benzaldehydes) **3a**, **3c**, and **3e** reacted with two equivalents of ethyl 2-(2-cyanoacetamido)-4,5,6,7-tetrahydrobenzo[*b*]thiophene-3-carboxylate **4** in ethanol in the presence of a few drops of piperidine at reflux for 30 min, condensation occurred from both sides with the two aldehydic groups and resulted in the formation of *bis*-ethyl 2-(2-cyanoacrylamido)-4,5,6,7-tetrahydrobenzo[*b*]thiophene-3-carboxylate derivatives **5**, **7**, and **9** respectively (Schemes 2 and 3). However, the reaction of bis(benzaldehydes) **3b**, **3d**, and **3f** with two equivalents of compound **4** afforded the respective ethyl 2-{2-cyano-3-[4-(4-formylphenoxy)alkoxy]phenyl} acrylamido-4,5,6,7-tetrahydrobenzo[*b*]thiophene-3-carboxylate derivatives **6**, **8**, and **10** in which condensation occurred from one side only (Schemes 2 and 3).

The chemical structures of the novel compounds **5–10** were proved spectroscopically on the basis of the elemental analysis and spectral data. The infrared (IR) spectrum of compound **5** as a representative example indicated the presence of NH group at 3,410 cm^{-1} and the carbonyl band at 1,662 cm^{-1}. The mass spectrum of compound **5** revealed a molecular ion peak as a base peak at *m/z* 818.

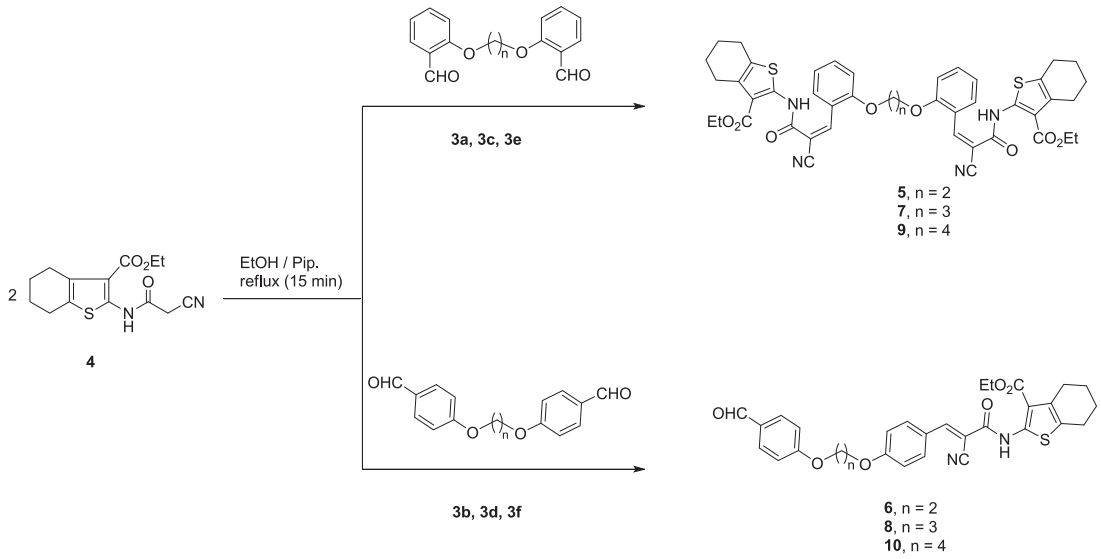

SCHEME 2 The synthesis of compounds **5–10**

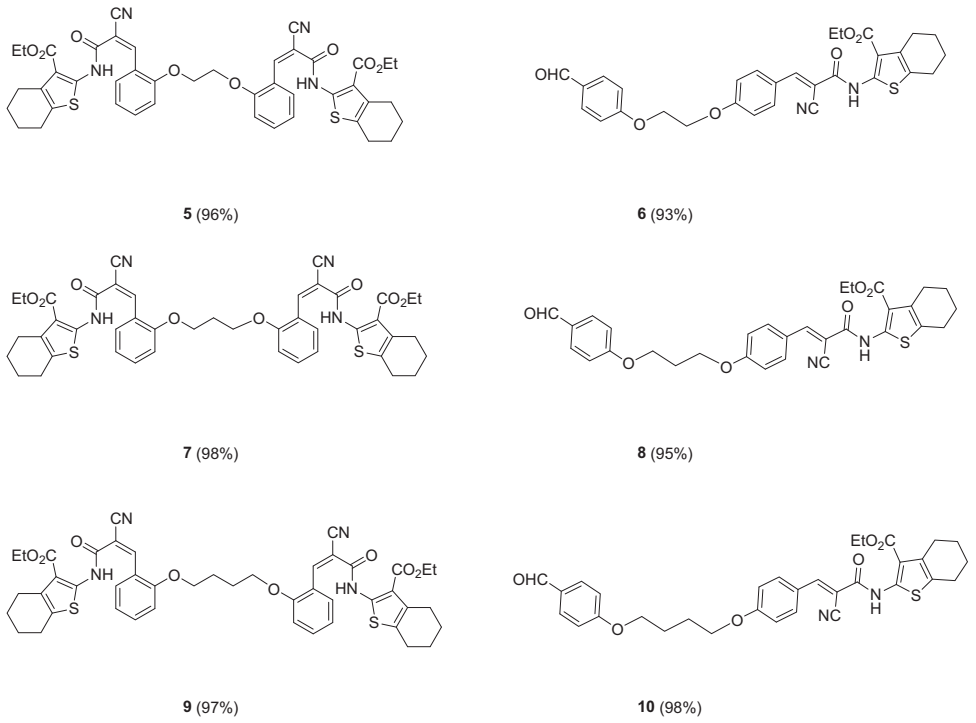

SCHEME 3 Structures of the prepared derivatives **5**–**10**

The ^{1}H nuclear magnetic resonance (NMR) spectrum indicated the ester group as multiplets at 1.30 and a quartet at 4.20 ppm. It showed the methylene linkage as multiplets at 4.57 ppm. It also revealed a singlet signal at 8.74 for the vinyl H3 proton. The amide NH group resonated at δ 11.68 ppm. All other signals appeared at their expected positions. On the contrary, the IR spectrum of compound **8** indicated the presence of NH group at 3,421 cm^{-1} and the carbonyl band at 1,667 cm^{-1}. The mass spectrum of compound **8** revealed a molecular ion peak as a base peak at *m/z* 558. The ^{1}H NMR spectrum indicated one ester group as multiplets at 1.34 and multiplets at 4.30 ppm. It also revealed a singlet signal integrated by one proton at 8.37 for the vinyl H3 proton. It featured one CHO group at 9.87 ppm. The amide NH group resonated at δ 11.95 ppm. All other signals appeared at their expected positions. Unfortunately, the ^{13}C NMR spectra of all the compounds, **5**–**10**, have not been assigned due to the poor solubility of these compounds in most of the deuterated solvents.

2.2 | Anticancer activity

2.2.1 | Primary screening

Compounds **5**–**10** were screened against three human cancer cell lines, namely Caucasian breast adenocarcinoma (MCF7), hepatocellular carcinoma (HEPG2), and colon cell line (HCT116), at 100 μg/ml, and their results were compared with the normal skin fibroblast cell line (BJ1). The results revealed that compounds **6**, **7**, **8**, **9**, and **10** exhibited more than 75% mortality against the HEPG2 cell line,

TABLE 1 % Mortality of cancer and normal cell lines at 100 μg/ml

Compounds	HEPG2	HCT116	MCF7	BJ1
5	68.2	42.5	47.6	55.3
6	76.2	42.6	49.5	35.4
7	100	54.3	49.5	51.4
8	80.1	11.3	42.6	10.5
9	100	65.6	52.6	5.3
10	75.3	64.6	51.8	22.4
Positive control	100	100	100	100
Negative control	0%	0%	0%	0%

TABLE 2 IC_{50} values (mM) for promising compounds

Compounds	HEPG2	HCT116	MCF7	BJ1
5	83.27	95.30	–	106.96
6	109.80	–	–	–
7	38.65	106.21	–	112.12
8	94.30	–	–	–
9	15.93	87.40	104.80	–
10	103.09	–	174.15	–
DOX	0.037	0.065	0.045	0.057
Negative control	0%	0%	0%	0%

Abbreviation: DOX, doxorubicin.

whereas compounds **7**, **9**, and **10** exhibited more than 50% mortality against HCT116. However, only two compounds, **9** and **10**, exhibited 50% mortality against MCF7, as shown in Table 1. So these promising compounds were subjected to secondary screening to calculate their IC_{50} values and selectivity index.

2.2.2 | Secondary screening

Concerning IC_{50} values, the most promising compounds for HEPG2 were compounds **9** and **7**, with IC_{50} values 15.93 and 38.65 mM, respectively. Compound **9** was found to be more promising than **7**,

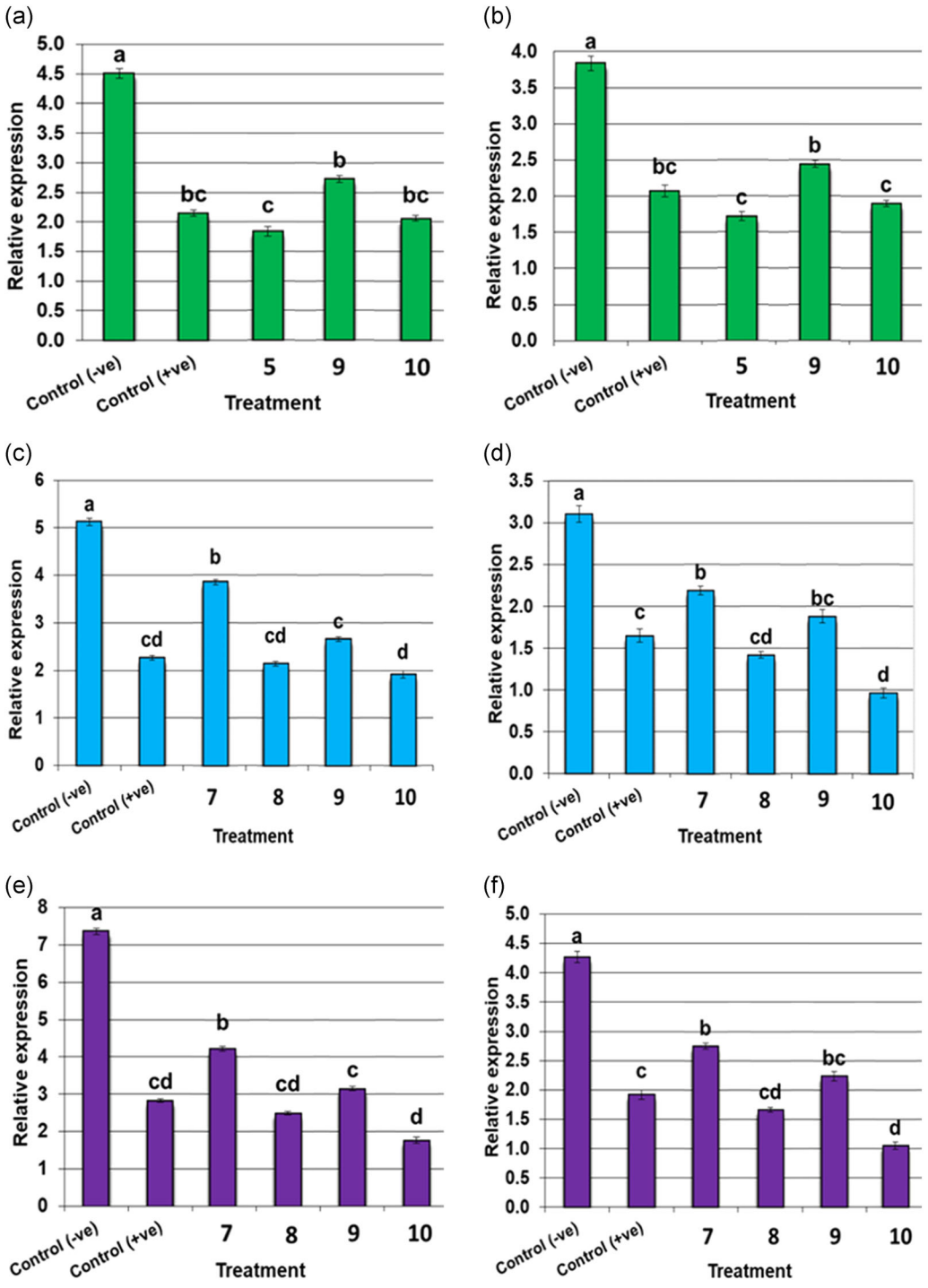

FIGURE 3 Alterations in the gene expression level of (a) COL10A1 and (b) COL11A1 genes in colon cancer cell line; (c) ESR1 and (d) ERBB2 genes in breast cancer cell line; and (e) AXIN1 and (f) CDKN2A genes in liver cancer cell line due to the treatment with the target molecules. Mean values with different superscript letters (a, b, c, and d) were significantly different ($p < .05$). Control (−ve): untreated and control (+ve): doxorubicin

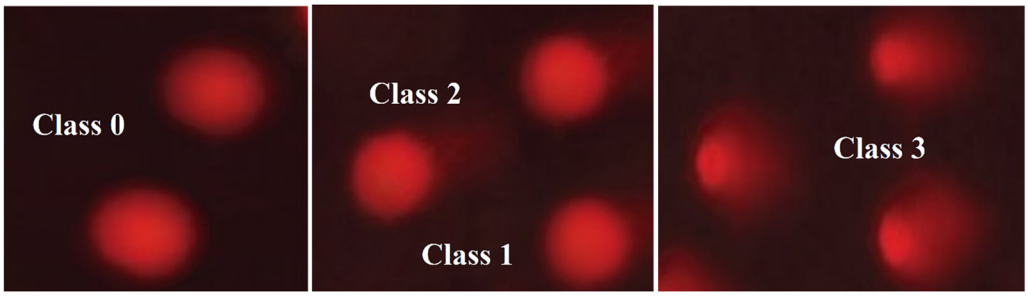

FIGURE 4 The visual score of normal DNA (Class 0) and damaged DNA (Classes 1, 2, and 3) using the comet assay in the investigated cell lines. Class 0, no tail; 1, tail length < diameter of nucleus; 2, tail length between 1× and 2× the diameter of nucleus; and 3, tail length > 2× the diameter of nucleus

where its selectivity index was higher than that of compound **9** and the values of IC_{50} ranged from 83.27 to 109.8 mM. However, in the case of MCF7 and HCT116 cell lines, compound **9** is still a promising compound, compared with others, but with a lower activity than for the HEPG2 cell line, as depicted in Table 2. This result elucidates that compound **9** exhibits selectivity against the HEPG2 cell line. Although the activity of compound **9** is lower than the chosen medicine, it has a higher selectivity index.

2.2.3 | Gene expression analysis

The gene expression analysis of colon cancer markers was carried out using two colon cancer-related genes, namely collagen type X α1 (COL10A1) and collagen type XI α1 (COL11A1). The results (Figure 3a,b) revealed that the COL10A1 and COL11A1 genes were found to be significantly overexpressed ($p < .05$) by about twofold in the negative control colon cancer cells, compared with the positive control (doxorubicin-treated). However, the expression values of these genes were decreased significantly in cells treated with compounds **5**, **9**, and **10**, compared with negative control cell lines, but they did not differ significantly from the positive control. However, the expression value of the COL10A1 gene was decreased significantly in compound **5**-treated cells, compared with compound **9**-treated cells. The expression value of the COL11A1 gene was decreased significantly in compounds **5**- and **10**-treated cells, compared with compound **9**-treated cells.

Moreover, the expression levels of estrogen receptors (ESR1) and Erb-B2 receptor tyrosine kinase 2 (ERBB2) genes were used as breast cancer markers, whereas the expression of AXIN1 and CDKN2A genes was used as a liver cancer marker. The expression of all the investigated breast and liver cancer markers in all treated and positive control cells was significantly ($p < .05$) lower than their expression in the negative control cells (Figure 3c–f). The expression of all the studied breast or liver cancer gene markers in the negative control cells was higher by around twofold than the positive control cell lines. Although the treatment with compound **7** decreased the expression level of the investigated breast and liver cancer markers, their expression was higher than in the positive controls.

Interestingly, the effects of the treatments with compounds **7**, **8**, **9**, and **10** on the expression of the breast cancer markers ESR1 and ERBB2, compared with liver cancer markers AXIN1 and CDKN2A, respectively, had several similarities. In the cells that were treated with compounds **8**, **9**, and **10**, the expression of ESR1 (in breast cancer cells) and AXIN1 (in liver cancer cells) was observed to be downregulated, with a significant similarity with the positive control cells. Additionally, compound **10**-treated cells had a significant lower expression values for ESR1 and AXIN1 genes, compared with compounds **7**- and **9**-treated cells (Figure 3c,e).

TABLE 3 The visual score of DNA damage in control and treated colon tumor cell lines

Treatment	No. of cells			No. of cells within each class				DNA damaged cells % (mean ± *SEM*)
	No. of samples	Analyzed	Comets	0	1	2	3	
Control (−ve)[d]	3	300	35	265	25	6	4	11.67 ± 0.76[c]
Control (+ve)[e]	3	300	71	229	32	21	18	23.65 ± 1.04[ab]
Compound **5**	3	300	74	226	20	33	21	24.71 ± 0.66[a]
Compound **9**	3	300	61	239	25	23	13	20.33 ± 0.72[b]
Compound **10**	3	300	72	228	26	22	24	24.11 ± 0.50[a]

Note: Mean values with different superscripts (a, b, and c) between locations in the same column are significantly different at $p < .05$.
Abbreviation: *SEM*, standard error of the mean.
[d]Untreated.
[e]Doxorubicin-treated.

TABLE 4 The visual score of DNA damage in control and treated breast tumor cell lines

	No. of cells			No. of cells within each class				
Treatment	No. of samples	Analyzed	Comets	0	1	2	3	DNA damaged cells % (mean ± *SEM*)
Control (−ve)[d]	3	300	26	274	19	5	2	8.67 ± 0.62[c]
Control (+ve)[e]	3	300	73	227	33	22	18	24.33 ± 0.76[a]
Compound **7**	3	300	53	247	21	20	12	17.66 ± 0.75[b]
Compound **8**	3	300	77	223	23	35	19	25.67 ± 0.53[a]
Compound **9**	3	300	69	231	27	22	20	23.00 ± 1.04[a,b]
Compound **10**	3	300	83	217	34	27	22	27.69 ± 0.78[a]

Note: Mean values with different superscripts (a, b, and c) between locations in the same column are significantly different at $p < .05$.
Abbreviation: *SEM*, standard error of the mean.
[d]Untreated.
[e]Doxorubicin-treated.

However, in cells treated with compounds **8** and **9**, the expression of ERBB2 (in breast cancer cells) and CDKN2A (in liver cancer cells) was observed to be downregulated, without significant differences as compared with the positive control. Cells treated with compound **10** had the significantly lowest ERBB2 and CDKN2A expression values among all treatments, except cells treated with compound **8** (Figure 3d,f).

2.2.4 | DNA damage using the comet assay

The DNA damage in colon, breast, and liver cancer cell lines was assessed by comet assay based on visual scores (from 0 to 3), as shown in Figure 4. In the colon cancer cell line (Table 3), the results revealed that negative cancer cell exhibited significantly lower ($p < .05$) DNA damage values, compared with the positive control (doxorubicin-treated cells). The DNA damage values were increased significantly in cell lines treated with compounds **5**, **9**, and **10**, compared with the negative control. Moreover, there were no significant differences between DNA damage values of cells treated with compounds **5**, **9**, and **10** and the positive control. Treatment with compounds **5** and **10** leads to significant higher DNA damage values than treatment with compound **9**.

Moreover, the comet assay results for the treated breast and liver cancer cell lines (Tables 4 and 5, respectively) showed that the positive control and all treated cells had a significantly ($p < .05$) higher DNA damage value than the negative control. The treatment with compound **7** had a lower DNA damage value as compared with the positive control and all treated cells, except those treated with compound **9**. However, there are no significant differences in the DNA damage value among the positive control and cells treated with compounds **8**, **9**, and **10**.

2.2.5 | DNA fragmentation assay

The rate of DNA fragmentation determined in colon cancer cell lines is summarized in Table 6 and Figure 5a. The results showed that the rate of DNA fragmentation was increased significantly ($p < .05$) in positive control (doxorubicin-treated) cancer cell lines, in addition to cell lines treated with compounds **5**, **9**, and **10**, compared with negative control cancer cell lines. Moreover, there were no

TABLE 5 The visual score of DNA damage in control and treated liver tumor cell lines

	No. of cells			No. of cells within each class				
Treatment	No. of samples	Analyzed	Comets	0	1	2	3	DNA damaged cells % (mean ± *SEM*)
Control (−ve)[d]	3	300	29	271	22	4	3	9.68 ± 0.61[c]
Control (+ve)[e]	3	300	76	224	34	24	18	25.32 ± 0.56[a]
Compound **7**	3	300	54	246	20	23	11	18.00 ± 0.72[b]
Compound **8**	3	300	79	221	22	36	21	26.33 ± 0.65[a]
Compound **9**	3	300	71	229	26	23	22	23.67 ± 0.94[a,b]
Compound **10**	3	300	85	215	33	29	23	28.33 ± 0.56[a]

Note: Mean values with different superscripts (a, b, and c) between locations in the same column are significantly different at $p < .05$.
Abbreviation: *SEM*, standard error of the mean.
[d]Untreated.
[e]Doxorubicin-treated.

TABLE 6 Detected DNA fragmentation in control and treated colon tumor cell lines

Treatment	DNA fragmentation % (mean ± *SEM*)	Change	Inhibition
Control (-ve)[d]	5.63 ± 0.1[c]	0	0
Control (+ve)[e]	21.72 ± 1.3[a,b]	16.1	0
Compound **5**	23.9 ± 1.26[a]	17.3	7.45
Compound **9**	18.41 ± 0.53[b]	12.8	−20.49
Compound **10**	22.13 ± 2.11[a]	16.5	2.48

Note: Mean values with different superscripts (a, b, and c) between locations in the same column are significantly different at $p < .05$.
Abbreviation: *SEM*, standard error of the mean.
[d]Untreated.
[e]Doxorubicin-treated.

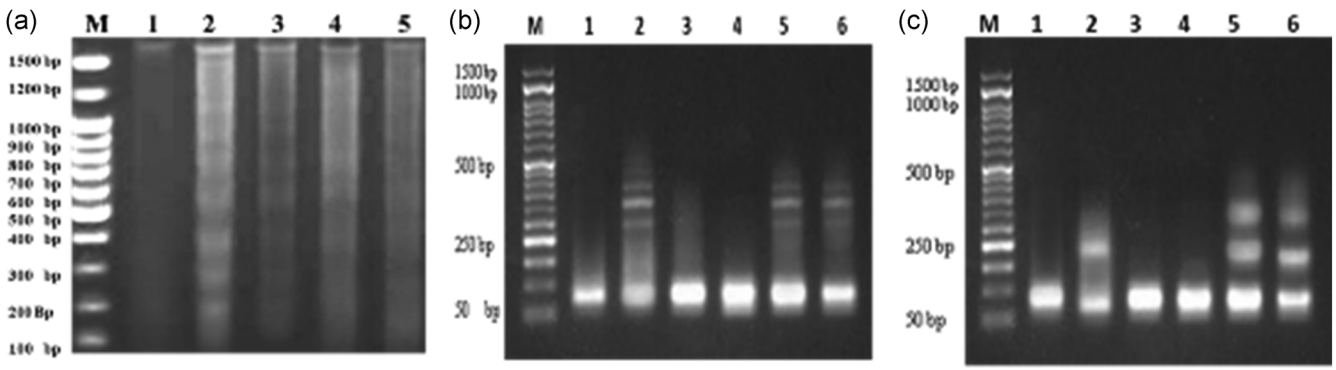

FIGURE 5 Detection of DNA fragmentation using agarose gel in (a) control and treated colon cancer, (b) breast cancer, (c) and liver cancer cell lines. In the three images, M, DNA marker; 1, control (−ve); 2, control (+ve). In image (a), 3, compound **9**; 4, compound **5**; and 5, compound **10**. In images (b) and (c), 3, compound **9**; 4, compound **7**; 5, compound **10**; and 6, compound **8**

significant differences between positive control cancer cell lines and cell lines treated with compounds **5**, **9**, and **10**, but the DNA damage values in cell lines treated with compounds **5** and **10** were significantly higher than those treated with compound **9**.

Furthermore, the effect of the treatments on the percentage of DNA fragmentation in the breast and liver cancer cell lines was investigated (Tables 7 and 8, respectively, and Figure 5b,c, respectively). The percentage of fragmented DNA in the positive control and breast and liver cancer cells treated with compounds **7**, **8**, **9**, and **10** was significantly high ($p < .05$), compared with the negative control cells. No significant differences were detected between the DNA damage value of cells treated with compounds **8**, **9**, and **10** and positive control cells, but the positive control cells and cells treated with compounds **8** and **10** had higher DNA damage values than those treated with compound **7**.

TABLE 7 Detected DNA fragmentation in control and treated breast tumor cell lines

Treatment	DNA fragmentation % (mean ± *SEM*)	Change	Inhibition
Control (−ve)[d]	6.4 ± 0.08[c]	0	0
Control (+ve)[e]	21.8 ± 1.1[a,b]	15.4	0
Compound **7**	15.9 ± 0.53[b]	9.5	−38.31
Compound **8**	24.1 ± 2.11[a]	17.7	14.93
Compound **9**	20.5 ± 1.3[a,b]	14.1	−8.44
Compound **10**	26.2 ± 1.26[a]	19.8	28.57

Note: Mean values with different superscripts (a, b, and c) between locations in the same column are significantly different at $p < .05$.
Abbreviation: *SEM*, standard error of the mean.
[d]Untreated.
[e]Doxorubicin-treated.

TABLE 8 Detected DNA fragmentation in control and treated liver tumor cell lines

Treatment	DNA fragmentation % (mean ± *SEM*)	Change	Inhibition
Control (−ve)[d]	5.9 ± 0.06[c]	0	0
Control (+ve)[e]	20.3 ± 0.09[a,b]	14.7	0
Compound **7**	14.8 ± 0.07[b]	10.1	−37.41
Compound **8**	23.4 ± 1.41[a]	18.3	15.63
Compound **9**	19.7 ± 1.3[a,b]	13.8	−9.33
Compound **10**	25.6 ± 1.52[a]	20.2	29.67

Note: Mean values with different superscripts (a, b, and c) between locations in the same column are significantly different at $p < .05$.
Abbreviation: *SEM*, standard error of the mean.
[d]Untreated.
[e]Doxorubicin-treated.

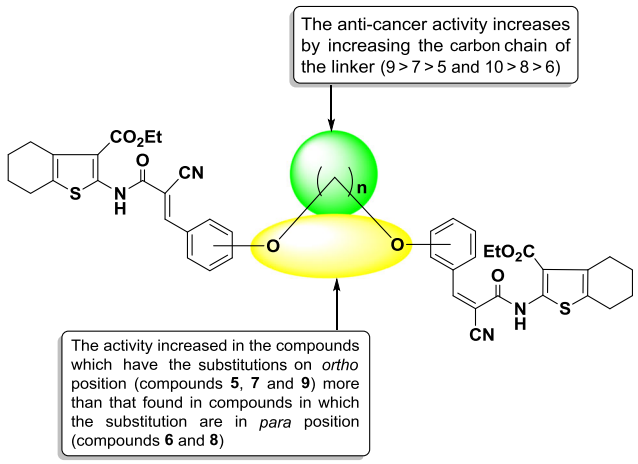

FIGURE 6 Structure–activity relationship of the prepared compounds **5**–**10**

2.3 | Structure–activity relationship (SAR)

The preliminary SAR of anticancer activity of compounds **5**–**10** is summarized and discussed in Figure 6. It is suggested that the linker length and the position of the cyanoacrylamide on the benzene ring were essential for the anticancer activity. The increase in the length of the linker was found to increase the activity of the compounds. Likewise, the activity increases in the compounds in which the cyanoacrylamide moieties are in the *ortho* position with respect to the alkoxy group and with *bis*-cyanoacrylamide moieties (**5**, **7**, and **9**), compared with those in which the groups are located in the *para* position with one cyanoacrylamide unit (**6**, **8**, and **10**).

3 | CONCLUSIONS

We could develop an efficient and simple method for the synthesis of *bis*-2-cyanoacetamide derivatives linked to the 4,5,6,7-tetrahydrobenzo[*b*]thiophene moiety. The structures of the novel compounds were established by the different spectral tools as well as the elemental analyses. All the promising compounds (**5**, **9**, **10** as anti-colon cancer and **7**, **8**, **9**, **10** as anti-breast and anti-liver cancer agents) reduced the expression levels of each type of cancer genetic marker and induced higher DNA damage levels, compared with the negative controls. Moreover, the anticancer activities of these compounds are comparable and in some cases superior to doxorubicin as a known anticancer drug.

4 | EXPERIMENTAL

4.1 | Chemistry

4.1.1 | General

All reactions were carried out in aerobic conditions at room temperature. Acetonitrile was distilled and kept under an inert atmosphere. All glassware was oven-dried at 120°C for at least 24 hr before use. 4-Tolylsulfonylisocyanate, 4-tolylisocyanate, benzoyl isocyanate, and ethyl isocyanate were purchased from Sigma-Aldrich and used as received. The starting materials, **3a**–**f**, have been prepared as described in the literature.[44-47] All melting points were uncorrected and measured using Electrothermal IA 9100 apparatus (Shimadzu, Japan). The IR spectra were recorded as potassium bromide pellets on a JASCO spectrophotometer between 4,000 and 400 cm^{-1}. ^1H NMR spectra (see the Supporting Information Data for the original spectra) were recorded in deuterated dimethylsulfoxide (DMSO)-d_6 on a Bruker spectrometer (400 MHz) at 25°C, but for compound **5**, it was recorded on a Varian spectrometer (300 MHz) at 30°C. The chemical shifts were expressed as part per million (δ values, ppm) using the solvent (DMSO = 2.51, water signal at 3.34) as the reference. Microanalyses were performed using Elementar Vario Cube apparatus and the mass spectra were recorded using Shimadzu Qp-2010 plus, Micro Analytical Center, Cairo University.

The InChI codes of the investigated compounds, together with some biological activity data, are provided as Supporting Information Data.

4.1.2 | General procedures for the synthesis of the bis(cyanoacrylamido) derivatives 5–10

Few drops of piperidine were added to a solution of ethyl 2-(2-cyanoacetamido)-4,5,6,7-tetrahydrobenzo[*b*]thiophene-3-carboxylate **4** (2 mmol) and bis(benzaldehydes) (**3a–f**) (1 mmol) in ethanol (15 ml). The reaction mixture was then heated at reflux for 30 min. The precipitate was filtered off and washed with hot ethanol (2 × 5 ml) and dried under vacuum to afford the products **5–10** as yellow solids.

*Diethyl 2,2′-({3,3′-[(ethane-1,2-diylbis(oxy))bis(2,1-phenylene)]bis(2-cyanoacryloyl)}bis(azanediyl))bis(4,5,6,7-tetrahydrobenzo[b]thiophene-3-carboxylate) (**5**)*

Yield 96%, Mp > 300°C. IR (KBr, cm^{-1}): 3,410 (NH), 1,662 (C═O), 2,215 (CN). ^{1}H NMR (300 MHz, DMSO-d_6): δ, ppm: 1.30 (m, 6H, CH_3), 1.72 (m, 8H, CH_2), 2.50–2.60 (m, 8H, CH_2), 4.20 (q, J = 6.9 Hz, 4H, CH_2), 4.57 (m, 4H, $2OCH_2$), 7.30 (m, 4H, Ar-H), 7.69 (m, 2H, Ar-H), 8.28 (d, J = 7.8 Hz, 2H, Ar-H), 8.74 (s, 2H, vinyl-H), 11.68 (s, 2H, NH). Anal. calcd. for $C_{44}H_{42}N_4O_8S_2$ (818.96): C, 64.53; H, 5.17; N, 6.84; found: C, 64.44; H, 5.26; N, 6.98%.

*Ethyl 2-(2-cyano-3-{4-[2-(4-formylphenoxy)ethoxy]phenyl}-acrylamide)-4,5,6,7-tetrahydrobenzo[b]thiophene-3-carboxylate (**6**)*

Yield 93%, Mp > 300°C. IR (KBr, cm^{-1}): 3,420 (NH), 1,665 (C═O), 2,210 (CN). ^{1}H NMR (400 MHz, DMSO-d_6): δ, ppm: 1.33 (m, 3H, CH_3), 1.73 (m, 4H, CH_2), 2.72 (m, 4H, CH_2), 4.34–4.51 (m, 6H, $2OCH_2 + CH_2CH_3$), 7.23 (m, 4H, Ar-H), 7.89 (m, 2H, Ar-H), 8.12 (m, Hz, 2H, Ar-H), 8.41 (s, 1H, vinyl-H), 9.88 (s, 1H, CHO), 11.88 (s, 1H, NH). MS: m/z 544 (M^+). Anal. calcd. for $C_{30}H_{28}N_2O_6S$ (544.62): C, 66.16; H, 5.18; N, 5.14; found: C, 66.37; H, 5.31; N, 5.32%.

*Diethyl 2,2′-({3,3′-[(propane-1,3-diylbis(oxy))bis(2,1-phenylene)]bis-(2-cyanoacryloyl)}bis(azanediyl))bis(4,5,6,7-tetrahydrobenzo[b]thiophene-3-carboxylate) (**7**)*

Yield 98%, Mp > 300°C. IR (KBr, cm^{-1}): 3,383 (NH), 2,825 (CH), 1,653 (C═O); ^{1}H NMR (400 MHz, DMSO-d_6): δ, ppm: 1.31 (m, 6H, CH_3), 1.74 (m, 6H, CH_2), 2.33 (m, 4H, CH_2), 2.64 (m, 8H, CH_2), 4.39 (m, 8H, $CH_2 + 2OCH_2$), 7.14–7.26 (m, 4H, Ar-H), 7.58 (m, 2H, Ar-H), 8.10 (m, 2H, Ar-H), 8.64 (m, 2H, vinyl-H), 11.92 (s, 2H, NH). Anal. calcd. for $C_{45}H_{44}N_4O_8S_2$ (832.99): C, 64.89; H, 5.32; N, 6.73; found: C, 65.25; H, 5.82; N, 6.25%.

*Ethyl 2-(2-cyano-3-{4-[3-(4-formylphenoxy)propoxy]phenyl}-acrylamido)-4,5,6,7-tetrahydrobenzo[b]thiophene-3-carboxylate (**8**)*

Yield 95%, Mp > 300°C. IR (KBr, cm^{-1}): 3,421 (NH), 2,829 (CH), 1,667 (C═O); ^{1}H NMR (400 MHz, DMSO-d_6): δ, ppm: 1.34 (m, 3H, CH_3), 1.74 (m, 4H, CH_2), 2.26 (m, 2H, CH_2), 2.73 (m, 4H, CH_2), 4.30 (m, 6H, $2OCH_2 + CH_2CH_3$), 7.18 (m, 4H, Ar-H), 7.88 (m, 2H, Ar-H), 8.08 (m, 2H, Ar-H), 8.37 (s, 1H, vinyl-H), 9.87 (s, 1H, CHO), 11.95 (s, 1H, NH). Anal. calcd. for $C_{31}H_{30}N_2O_6S$ (558.65): C, 66.65; H, 5.41; N, 5.01; found: C, 66.82; H, 5.59; N, 5.14%.

*Diethyl 2,2′-({3,3′-[(butane-1,4-diylbis(oxy))bis(2,1-phenylene)]bis-(2-cyanoacryloyl)}bis(azanediyl))bis(4,5,6,7-tetrahydrobenzo[b]thiophene-3-carboxylate) (**9**)*

Yield 97%, Mp > 300°C. IR (KBr, cm^{-1}): 3,398 (NH), 2,823 (CH), 1,656 (C═O); ^{1}H NMR (400 MHz, DMSO-d_6): δ, ppm: 1.32 (m, 6H, CH_3), 1.74 (m, 8H, CH_2), 2.01 (m, 4H, CH_2), 2.70 (m, 8H, CH_2), 4.30 (m, 8H, CH_2), 7.04–7.23 (m, 4H, Ar-H), 7.64 (m, 2H, Ar-H), 8.15 (m, 2H, Ar-H), 8.69 (s, 2H, vinyl-H), 10.34 (s, 2H, 2 NH). Mass spectroscopy (MS): m/z 847 (M^+). Anal. calcd. for $C_{46}H_{46}N_4O_8S_2$ (847.01): C, 65.23; H, 5.47; N, 6.61; found: C, 65.42; H, 5.95; N, 6.83%.

*Ethyl 2-(2-cyano-3-{4-[4-(4-formylphenoxy)butoxy]phenyl}acryl-amido)-4,5,6,7-tetrahydrobenzo[b]thiophene-3-carboxylate (**10**)*

Yield 98%, Mp > 300°C. IR (KBr, cm^{-1}): 3,418 (NH), 2,875 (CH), 1,663 (C═O); ^{1}H NMR (400 MHz, DMSO-d_6): δ, ppm: 1.30 (m, 3H, CH_3), 1.75 (m, 4H, CH_2), 2.27 (m, 4H, CH_2), 2.68 (m, 4H, CH_2), 4.30 (m, 6H, $CH_2 + 2OCH_2$), 7.19 (m, 4H, Ar-H), 7.89 (m, 2H, Ar-H), 8.11 (m, 2H, Ar-H), 8.40 (s, 1H, vinyl-H), 9.88 (s, 1H, CHO), 11.97 (s, 1H, NH). Anal. calcd. for $C_{32}H_{32}N_2O_6S$ (572.68): C, 67.12; H, 5.63; N, 4.89; found: C, 67.23; H, 5.78; N, 4.97%.

4.2 | Anticancer evaluation

4.2.1 | Materials and methods

The MTT (3-(4,5-dimethylthiazol-2-yl)-2,5-diphenyl tetrazolium bromide) assay developed by Mosmann was modified by Miura and used to determine the in vitro inhibitory effects of the test compounds on cell growth. Briefly, a medium containing 10×10^3 cells (HEPG2, HCT-116, MCF-7, and BJ1 cells) in a fresh complete growth medium was seeded into each well of a 96-well microplate, with the compound solution added simultaneously to triplicate wells, before the final volume was made up to 100 ml. The plate was incubated at 37°C for 72 hr in a humidified atmosphere of 5% CO_2 using a water-jacketed carbon dioxide incubator (TC2323; Sheldon, Cornelius, OR). The medium was aspirated, fresh medium (without serum) was added, and cells were incubated, either alone (negative control) or with different concentrations of the sample, to give a final concentration of 100, 50, 25, 12.5, 6.25, 3.125, 1.56, and 0.78 mg/ml. Cells were suspended in an RPMI-1640 medium for HEPG2, MCF-7, and HCT-116, and DMEM-F12 for BJ1, 1% antibiotic–antimycotic mixture (10,000 U/ml potassium penicillin, 10,000 mg/ml streptomycin sulfate, and 25 mg/ml amphotericin B) and 1% L-glutamine in a 96-well flat-bottom microplate at 37°C under 5% CO_2. After 48 hr of incubation, the medium was aspirated; 200 ml of 10% sodium dodecyl sulfate (SDS) in deionized water was added to each well and further incubated overnight at 37°C under 5% CO_2. Then, 200 ml of 10% SDS in deionized water was added to each well to stop the reaction and to solubilize any MTT formazan that had formed, and then it was incubated overnight at 37°C. Doxorubicin, which is a known natural cytotoxic agent, was used as a positive control

(100 mg/ml), which exhibited 100% lethality under the same conditions. Also, 100 ml of 0.02 N HCl/50% *N,N*-dimethylformamide, 20% SDS was added to solubilize any MTT formazan that had formed. The optical density of each well was measured at 575 nm (OD575) using a microplate multiwell reader (model 3350; Bio-Rad Laboratories Inc., Hercules, CA), and the inhibition of cell growth (%) was calculated as $(1 - T/C) \times 100$, where C is the mean OD575 of the control group and T is that of the treated group. The IC_{50} value was determined from the dose–response curve. Statistical significance was tested between samples and negative control (cells with vehicle) using independent *t*-test by SPSS 11 program (Chicago, IL).

4.2.2 | The gene expression analysis

RNA isolation

RNeasy Mini Kit (Qiagen, Hilden, Germany) was used to extract total RNA from each type of treated and control cancer cell line following the kit manual, and then a treatment was applied using RNAse-free DNAse (Invitrogen, Germany) to eliminate any DNA contamination. Whereas the RNA integrity was checked by formaldehyde-containing agarose gel electrophoresis, its quantity and purity were assessed photospectrometrically at 260 nm and by 260/280 nm ratio, respectively. Then, the extracted RNA aliquots were stored at −80°C.

Reverse-transcription (RT) reaction

The RT reactions were performed for the isolated messenger RNA from the treated and control cancer cell lines using RevertAid™ First Strand cDNA Synthesis Kit (Fermentas, Germany). The kit's manual instructions for the reaction setup and incubation were followed for a reaction with 20 µl total volume that contained oligo-dT as a primer and 5 µg of RNA. Afterward, the complementary DNA (cDNA) samples were stored at −80°C.

Quantitative real-time PCR (qPCR)

The expression levels of the studied genes were quantified within the treated and control cancer cell lines using StepOne™ Real-Time PCR System (Thermo Fisher Scientific, Waltham, MA). Real-time reverse-transcription polymerase chain reaction (qRT-PCR) reactions were performed with a total volume of 25 µl, consisting of 12.5 µl 1× SYBR® Premix Ex Taq™ (TaKaRa, Biotech Co. Ltd.), 0.5 µl of forward and reverse primer pairs (0.2 µM each) that are specific for each gene (Table 9), 6.5 µl ddH_2O, and 5 µl of cDNA reaction. qRT-PCR program was divided into three stages. The first stage occurred at 95.0°C for 3 min. The second stage consisted of 40 cycles in which each cycle was divided into three steps: 95.0°C for 15 s, the annealing temperature of each primer pair (Table 9) for 30 s and finally 72.0°C for 30 s. At the end, a gradient dissociation protocol (0.5°C every 30 s from 65°C to 95°C) was used to examine the specificity of the qPCR primers and the occurrence of primer dimers. Each trial involved ddH_2O as a control. The relative expression quantification of the target gene to the reference gene β-actin was determined by using the $2^{-\Delta\Delta C_t}$ method.

TABLE 9 Primer sequences used for RT-qPCR

Gene	Forward	Reverse	Annealing temp. (°C)	References
β-Actin	CTGGAACGGTGAAGGTGACA	CGGCCACATTGTGAACTTTG	56	[48]
Collagen type X α1 (COL10A1)	TCTCTAACTCTACCCCACCCTACAA	TACGTTTTTACGTTGCTGCTCACT	58	
Collagen type XI α1 (COL11A1)	ACGCTGCATATACAGGTACCATTTAG	TCAGCCCTGTTTCCATCTTAGC	59	
Estrogen receptor 1 (*ESR1*)	ATCTCGGTTCCGCATGATGAATCTGC	TGCTGGACAGAAATGTGTACACTCCAGA	62	[49]
ERBB2: Erb-B2 receptor tyrosine kinase 2 (*ERBB2*)	TGACCTGCTGGAAAAGGGGGAGCG	TCCCTGGCCATGCGGGAGAATTCAG	66	
Axis inhibition protein 1 (AXIN1)	CTCGGGTGTGTGAAAGCTC	ATTGTGTGGTCTGTGGAGGA	56	[50]
Cyclin-dependent kinase inhibitor 2A (CDKN2A)	GGCTGAACTTTCTGTGCTGG	CCCTTTGCTATTTTGCCCGT	56	

Abbreviation: RT-qPCR, quantitative reverse-transcription polymerase chain reaction.

4.2.3 | DNA damage using the comet assay

The neutral comet assay was performed according to the following protocol[51] for the treated and control cancer cell lines. In brief, a single-cell suspension was produced by trypsinization of each cell line plate. About 1.5×10^4 cells were fixed in 0.75% low-melting temperature agarose and placed on a precoated microscope slide, and the cells were lysed using the lysis buffer (0.5% SDS, 30 mM ethylenediaminetetraacetic acid [EDTA], pH 8.0) for 4 hr at 50°C. Then, the slides were rinsed overnight at room temperature in Tris/borate/EDTA buffer, pH 8.0, and the slides were subjected to electrophoresis at 0.6 V/cm for 25 min. Further, the slides were stained by propidium iodide. In total, 300 cells were studied to detect the ratio of cells with DNA damage. The cells were classified as follows: Class 0, no detectable DNA damage and no tail; Class 1, tail with a length < the diameter of the nucleus; Class 2, tail with length between 1× and 2× the nuclear diameter; and Class 3, tail longer than 2× the diameter of the nucleus.[52]

4.2.4 | DNA fragmentation assay

The cancer cell lines were treated with the investigated compounds, and then the cells were trypsinized and washed with Dulbecco's phosphate-buffered saline. The cells were treated for 30 min on ice by a lysis buffer (10 mM Tris [pH 7.4], 150 mM NaCl, 5 mM EDTA, and 0.5% Triton X-100). The cell lysates were centrifuged for 20 min at 10,000*g*. An equal volume of neutral phenol/chloroform/:isoamyl alcohol mixture (25:24:1) was added to supernatant to extract the fragmented DNA and 2.5 volume of ethanol was used to precipitate the DNA. The pellet was dried and dissolved in TE buffer. The DNA was examined by electrophoresis on 2% agarose gels containing 0.1 μg/ml ethidium bromide.

CONFLICTS OF INTERESTS

The authors declare that there are no conflicts of interests.

ORCID

Farid M. Sroor http://orcid.org/0000-0003-1283-2157
Ahmed H. M. Elwahy http://orcid.org/0000-0002-3992-9488
Ismail A. Abdelhamid http://orcid.org/0000-0003-1220-8370

REFERENCES

[1] World Cancer Report 2014. http://publications.iarc.fr/Non-Series-Publications/World-Cancer-Reports/World-Cancer-Report-2014
[2] W. S. Wang, X. L. Zhu, X. Q. Hong, L. Zheng, H. Zhu, Y. Z. Hu, *MedChemComm* **2013**, *4*, 411.
[3] J. Balzarini, J. Thomas, S. Liekens, S. Noppen, W. Dehaen, R. Romagnoli, *Invest. New Drug* **2014**, *32*, 200.
[4] J. Thomas, A. Jejcic, P. Vervaeke, R. Romagnoli, S. Liekens, J. Balzarini, W. Dehaen, *ChemMedChem* **2014**, *9*, 2744.
[5] A. M. Isloor, B. Kalluraya, K. Sridhar Pai, *Eur. J. Med. Chem.* **2010**, *45*, 825.
[6] C. Mugnaini, A. Rabbito, A. Brizzi, N. Palombi, S. Petrosino, R. Verde, V. Di Marzo, A. Ligresti, F. Corelli, *Eur. J. Med. Chem.* **2019**, *161*, 239.
[7] H. M. Aly, N. M. Saleh, H. A. Elhady, *Eur. J. Med. Chem.* **2011**, *46*, 4566.
[8] M. Hrast, S. Turk, I. Sosič, D. Knez, C. P. Randall, H. Barreteau, C. Contreras-Martel, A. Dessen, A. J. O'Neill, D. Mengin-Lecreulx, D. Blanot, S. Gobec, *Eur. J. Med. Chem.* **2013**, *66*, 32.
[9] C. Núñez, J. Fernández-Lodeiro, A. Fernández-Lodeiro, E. Bértolo, J. L. Capelo, C. Lodeiro, *Molbank* **2012**, *2012*, M768.
[10] J. Thomas, A. Jecic, E. Vanstreels, L. van Berckelaer, R. Romagnoli, W. Dehaen, S. Liekens, J. Balzarini, *Eur. J. Med. Chem.* **2017**, *132*, 219.
[11] S. Saxena, G. Samala, J. P. Sridevi, P. B. Devi, P. Yogeeswari, D. Sriram, *Eur. J. Med. Chem.* **2015**, *92*, 401.
[12] S. Massari, G. Nannetti, L. Goracci, L. Sancineto, G. Muratore, S. Sabatini, G. Manfroni, B. Mercorelli, V. Cecchetti, M. Facchini, G. Palù, G. Cruciani, A. Loregian, O. Tabarrini, *J. Med. Chem.* **2013**, *56*, 10118.
[13] G. Muratore, L. Goracci, B. Mercorelli, Á. Foeglein, P. Digard, G. Cruciani, G. Palù, A. Loregian, *Proc. Natl. Acad. Sci. U. S. A.* **2012**, *109*, 6247.
[14] M. F. Mohamed, Y. M. Attia, S. A. Shouman, I. A. Abdelhamid, *Anti-Cancer Agents Med. Chem.* **2017**, 17.
[15] M. F. Mohamed, N. Samir, A. Ali, N. Ahmed, Y. Ali, S. Aref, O. Hossam, M. S. Mohamed, A. M. Abdelmoniem, I. A. Abdelhamid, *Bioorg. Chem.* **2017**, *73*, 43.
[16] S. K. Salama, M. F. Mohamed, A. F. Darweesh, A. H. M. Elwahy, I. A. Abdelhamid, *Bioorg. Chem.* **2017**, *71*, 19.
[17] M. Y. Karimi, I. Fatemi, H. Kalantari, M. A. Mombeini, S. Mehrzadi, M. Goudarzi, *J. Diet. Suppl.* **2019**, 1. https://doi.org/10.1080/19390211.2019.1634175
[18] M. A. Gouda, M. A. Berghot, G. E. Abd El-Ghani, A. M. Khalil, *Eur. J. Med. Chem.* **2010**, *45*, 1338.
[19] K. Onda, R. Shiraki, Y. Yonetoku, K. Momose, N. Katayama, M. Orita, T. Yamaguchi, M. Ohta, S. Tsukamoto, *Bioorg. Med. Chem.* **2008**, *16*, 8627.
[20] Z.-L. Ren, H. Liu, D. Jiao, H.-T. Hu, W. Wang, J.-X. Gong, A.-L. Wang, H.-Q. Cao, X.-H. Lv, *Drug Dev. Res.* **2018**, *79*, 307.
[21] W. D. Easterly, M. W. Jordin, W. S. Dorsey, G. Clark, *J. Pharm. Sci.* **1965**, *54*, 1358.
[22] J. Fu, K. Cheng, Z.-m Zhang, R.-q Fang, H.-l Zhu, *Eur. J. Med. Chem.* **2010**, *45*, 2638.
[23] M. Yusuf, P. Jain, *J. Chem. Sci.* **2013**, *125*, 117.
[24] A. C. Véras Of Aguiar, R. O. Of Moura, J. F. Bezerra Mendonça, H. A. de Oliveira Rocha, R. B. Gomes Câmara, M. dos Santos Carvalho Schiavon, *Biomed. Pharmacother.* **2016**, *84*, 403.
[25] T. Hagemann, J. Winsberg, B. Haupler, T. Janoschka, J. J. Gruber, A. Wild, U. S. Schubert, *NPG Asia Mater.* **2017**, *9*.
[26] J. Y. Li, S. X. Yang, L. Wang, X. B. Wang, L. Liu, *Macromolecules* **2013**, *46*, 6832.
[27] T. Boyiri, M. K. Safo, R. E. Danso-Danquah, J. Kister, C. Poyart, D. J. Abraham, *Biochemistry* **1995**, *34*, 15021.
[28] J.-Y. Choi, Y. V. Surovtseva, S. M. Van Sickle, J. Kumpf, U. H. F. Bunz, C. Ben Mamoun, D. R. Voelker, *J. Biol. Chem.* **2018**, *293*, 1493.
[29] T. Kaur, R. N. Gautam, A. Sharma, *Chem. Asian J.* **2016**, *11*, 2938.
[30] A. Hafeez, Z. Akhter, J. F. Gallagher, N. A. Khan, A. Gul, F. U. Shah, *Polymers* **2019**, *11*, 1498.
[31] D. Sysoiev, C. Barnes, T. Huhn, *Chem. Heterocycl. Compd.* **2019**, *55*, 792.
[32] J. Akhigbe, L. P. Samankumara, C. Brückner, *Tetrahedron Lett.* **2012**, *53*, 3524.
[33] S. D. Joshi, S. R. P. Kumar, S. Patil, M. Vijayakumar, V. H. Kulkarni, M. N. Nadagouda, A. M. Badiger, C. Lherbet, T. M. Aminabhavi, *Med. Chem. Res.* **2019**, *28*, 1838.
[34] H. M. Diab, W. M. I. Hassan, I. A. Abdelhamid, A. H. M. Elwahy, *J. Mol. Struct.* **2019**, *1197*, 244.
[35] F. M. Saleh, H. M. Hassaneen, A. M. Abdelmoniem, A. H. M. Elwahy, I. A. Abdelhamid, *J. Heterocycl. Chem.* **2019**, *56*, 1914.
[36] M. A. Tantawy, F. M. Sroor, M. F. Mohamed, M. E. El-Naggar, F. M. Saleh, H. M. Hassaneen, I. A. Abdelhamid, *Anti-Cancer Agents Med. Chem.* **2019**, *20*, 70.

[37] F. M. Sroor, S. Y. Abbas, W. M. Basyouni, K. A. M. El-Bayouki, M. F. El-Mansy, H. F. Aly, S. A. Ali, A. F. Arafa, A. A. Haroun, *Bioorg. Chem.* **2019**, *92*, 103290.
[38] F. M. Sroor, A. M. Abdelmoniem, I. A. Abdelhamid, *ChemistrySelect* **2019**, *4*, 10113.
[39] F. M. Sroor, T. K. Khatab, W. M. Basyouni, K. A. M. El-Bayouki, *Synthetic Commun.* **2019**, *49*, 1444.
[40] F. M. Sroor, C. G. Hrib, L. Hilfert, L. Hartenstein, P. W. Roesky, F. T. Edelmann, *J. Organomet. Chem.* **2015**, *799–800*, 160.
[41] M. E. Salem, M. Hosny, A. F. Darweesh, A. H. M. Elwahy, *Synth. Commun.* **2019**, *49*, 2319.
[42] A. M. S. Hebishy, I. A. Abdelhamid, A. H. M. Elwahy, *Arkivoc* **2018**, *2018*, 97.
[43] F. M. Sroor, W. M. Basyouni, W. M. Tohamy, T. H. Abdelhafez, M. K. El-awady, *Tetrahedron* **2019**, *75*, 130749. https://doi.org/10.1016/j.tet.2019.130749
[44] O. M. Sayed, A. E. M. Mekky, A. M. Farag, A. H. M. Elwahy, *J. Sulfur Chem.* **2015**, *36*, 124.
[45] A. E. M. Mekky, A. F. Darweesh, A. A. Salman, A. M. Farag, *Heterocycles* **2014**, *89*, 1827.
[46] H. A. Muathen, N. A. M. Aloweiny, A. H. M. Elwahy, *J. Heterocycl. Chem.* **2009**, *46*, 656.
[47] A. H. M. Elwahy, *Tetrahedron* **2000**, *56*, 897.
[48] Q. Yang, M. H. Feng, X. Ma, H. C. Li, W. Xie, *Oncol. Lett.* **2017**, *14*, 6071.
[49] P. Potemski, E. Pluciennik, A. K. Bednarek, R. Kusinska, R. Kubiak, R. Kordek, *Histopathology* **2007**, *51*, 829.
[50] Z. Qiu, K. Zou, L. Zhuang, J. Qin, H. Li, C. Li, Z. Zhang, X. Chen, J. Cen, Z. Meng, H. Zhang, Y. Li, L. Hui, *Sci. Rep.* **2016**, *6*.
[51] P. L. Olive, J. P. Banáth, R. E. Durand, *Radiat. Res.* **2012**, *178*, AV35.
[52] A. Collins, M. Dusinska, M. Franklin, M. Somorovska, H. Petrovska, S. Duthie, L. Fillion, M. Panayiotidis, K. Raslova, N. Vaughan, *Environ. Mol. Mutagen.* **1997**, *30*, 139.

SUPPORTING INFORMATION

Additional supporting information may be found online in the Supporting Information section.

How to cite this article: Sroor FM, Aboelenin MM, Mahrous KF, Mahmoud K, Elwahy AHM, Abdelhamid IA. Novel 2-cyanoacrylamido-4,5,6,7-tetrahydrobenzo[*b*]thiophene derivatives as potent anticancer agents. *Arch Pharm.* 2020;e2000069. https://doi.org/10.1002/ardp.202000069